Methods 76 (2015) 194–200

Contents lists available at ScienceDirect

Methods

journal homepage: www.elsevier.com/locate/ymeth

# Enzyme kinetics determined by single-injection isothermal titration calorimetry

Mark K. Transtrum [a], Lee D. Hansen [b,*], Colette Quinn [c]

[a] Department of Physics and Astronomy, Brigham Young University, Provo, UT 84602, USA
[b] Department of Chemistry and Biochemistry, Brigham Young University, Provo, UT 84602, USA
[c] Applications Lab, TA Instruments, Lindon, UT 84042, USA

ARTICLE INFO

*Article history:*
Received 26 November 2014
Accepted 1 December 2014
Available online 10 December 2014

*Keywords:*
Michaelis–Menten
Briggs–Haldane
Calorimetry
Time constant
Enthalpy
ITC

ABSTRACT

The purposes of this paper are (a) to examine the effect of calorimeter time constant ($\tau$) on heat rate data from a single enzyme injection into substrate in an isothermal titration calorimeter (ITC), (b) to provide information that can be used to predict the optimum experimental conditions for determining the rate constant ($k_2$), Michaelis constant ($K_M$), and enthalpy change of the reaction ($\Delta_R H$), and (c) to describe methods for evaluating these parameters. We find that $K_M$, $k_2$ and $\Delta_R H$ can be accurately estimated without correcting for the calorimeter time constant, $\tau$, if ($k_2E/K_M$), where $E$ is the total active enzyme concentration, is between $0.1/\tau$ and $1/\tau$ and the reaction goes to at least 99% completion. If experimental conditions are outside this domain and no correction is made for $\tau$, errors in the inferred parameters quickly become unreasonable. A method for fitting single-injection data to the Michaelis–Menten or Briggs–Haldane model to simultaneously evaluate $K_M$, $k_2$, $\Delta_R H$, and $\tau$ is described and validated with experimental data. All four of these parameters can be accurately inferred provided the reaction time constant ($k_2E/K_M$) is larger than $1/\tau$ and the data include enzyme saturated conditions.



## 1. Introduction

Mass-action kinetic models, of which Michaelis–Menten (or Briggs–Haldane) is one example, Eq. (1),

$$dS/dt = -k_2 ES/(K_M + S) \quad (1)$$

describe the kinetics of reactions catalyzed by a single enzyme and provide an approximation to the kinetics of processes involving a network of enzymes [1]. These models express the reaction rate as a function of the total concentration of active enzyme ($E$) and the concentration of substrate ($S$) with rate constants ($k_2$ or $k_{cat}$ in some literature) and mass-action constants ($K_M$) as parameters to be evaluated from the data. These functions do not have a simple closed form for the expression for $dS/dt = f(t)$ where $f(t)$ is a function of time. Therefore, equations with rate expressed as a function of time, which is the data form produced by heat-conduction and power-compensation isothermal titration calorimetry (ITC), cannot be obtained. This makes ITC data analysis with mass-action kinetic models particularly challenging.

Two ITC methods for determining enzyme kinetics have been described in the literature [2–4]; a multiple-injection method and a single-injection method. In the multiple injection method, the steady-state heat rate is measured after each injection of substrate into an enzyme solution. The data produced is a plot of heat rate versus concentration of substrate, typically with (20–40) data points. Since each data point takes 3–5 min, a single experiment takes 1.5–3.5 h. For this method to work, concentrations of enzyme and substrate must be adjusted so that heat rates change significantly with each injection of substrate but are also constant after each injection. The inverse titration is not practical because of leakage of enzyme from the burette after the first injection. In addition to the step-wise heat rate measurements, an additional single injection experiment must be done to determine the enthalpy change for the catalyzed reaction ($\Delta_R H$). Because $\tau$ does not enter into the calculation, after correction for the baseline and determination of $\Delta_R H$, evaluation of $K_M$ and $k_2$ from multiple-injection data can be done in a spreadsheet by the traditional methods used with the Michaelis–Menten model.

In the single-injection method, a single injection of enzyme is made into a solution of substrate with the substrate concentration adjusted so that the substrate is mostly consumed in 30 min to an hour. The data produced thus consists of several hundred measurements of heat rate versus time. Data from a single injection exper-

* Corresponding author. Fax: +1 801 422 0153.
*E-mail addresses:* mktranstrum@byu.edu (M.K. Transtrum), lee_hansen@BYU.edu (L.D. Hansen), cquinn@tainstruments.com (C. Quinn).

http://dx.doi.org/10.1016/j.ymeth.2014.12.003
1046-2023/

iment are shown by the solid line in Fig. 1. Since only one injection is necessary, leakage from the burette prior to injection can be prevented by filling the tip with a small amount of buffer. Although the single-injection method requires only one experiment, is significantly faster, and requires less enzyme, it has been little used because data analysis is significantly more challenging than analysis of multiple-injection data. Accurate analysis of single-injection data requires recursive, simultaneous fitting of the entire curve with $K_M$, $k_2$, $\Delta_R H$, $\tau$ and possibly the baseline heat rate, $\phi_B$, as fitting parameters.

The traditional method for correcting for instrument time constant by use of the Tian equation, e.g. [5,6],

$$\phi_{\text{corrected}} = \phi_{\text{measured}} + \tau(\mathrm{d}\phi_{\text{measured}}/\mathrm{d}t) \tag{2}$$

where $\tau$ is defined by the function $1 - e^{-t/\tau}$ for an increasing response and $e^{-t/\tau}$ for a decreasing response and $\phi$ is heat rate, presupposes an accurate value for $\tau$ that is not easily measured in heat-conduction and power-compensation calorimeters [7]. There is no universal value of $\tau$ for a particular calorimeter design, and since $\tau$ depends on the mixing time, thermal conductivity of the solution, and thermal time constants of all the parts of, and connections to, the reaction vessel, the value of $\tau$ is not the same for all calorimeters of the same design, and can vary from experiment to experiment even in the same calorimeter. Determination of $\tau$ by injection of methanol in a separate experiment or with a heater pulse prior to or post experiment produce values that differ significantly from the applicable value of $\tau$. For example, a heater pulse in the ITC model 2G used to collect the data in Fig. 1 gives $\tau = 12$ s, but analysis of the data by fitting to the model gives $\tau = 37$ s. In another example, the "high feedback response time" in the specifications for the MicroCal ITC 200 is 10 s (i.e., $\tau = 2$ s), but Burnouf et al. [8] report finding $\tau = 3.5$ s which gives a 99% response time of 18 s. Demarse et al. [9] found $\tau = 14.5$ s by fitting single injection data for sucrose–invertase from a NanoITC Low Volume instrument, but electrical heater pulse gave $\tau = 2.2$ s. Note that in every case, the value of $\tau$ obtained from a heater pulse is significantly shorter than the value of $\tau$ obtained from fitting kinetic data.

The mathematics necessary for multi-parametric fitting of single-injection data to a Michaelis–Menten model, Eqs. (3)–(6),

$$\phi_r(t) = -\Delta_R H V k_2 E S(t)/[K_M + S(t)] \tag{3}$$

$$-K_M \ln S - S = k_2 E t - K_M \ln S_0 - S_0 \tag{4}$$

$$t(S) = -(k_2 E)^{-1}[(S - S_0) + K_M \ln(S/S_0)] \tag{5}$$

$$\phi_{\text{cal}}(t) = \tau^{-1} e^{-t/\tau} \int e^{S/\tau} \phi_r(S)\mathrm{d}S \tag{6}$$

where $\phi_r$ is the heat rate from the reaction and $\phi_{\text{cal}}$ is the heat rate measured by the calorimeter, has been published [7,9] along with the process for use of these equations. The model in Eqs. (3)–(6) is fit to data by nonlinear least squares. First, the parameters $k_2$, $K_M$, $|\Delta_R H|$, and $\tau$ are log transformed. This guarantees that the parameter values remain positive and improves the efficiency of the fitting procedure. The resulting model is fit using the geodesic Levenberg–Marquardt algorithm [10,11]. The data to be fit do not contain error bars since each point consists of a single measurement. Assuming the error in each data point is from a Gaussian distribution with variance $\sigma^2$, we estimate $\sigma$ using a maximum likelihood method. If SS represents the sum of squares error from fitting the model, $\sigma^2 = \text{SS/M}$, where M is the number of independent data points in the sample. We find that $\sigma \approx 0.05$ for the data in Fig. 1. An alternative to this method uses the Lambert $W(x)$ (or Omega) function [12].

Use of ITC for determination of the kinetics of enzyme catalyzed reactions is increasing [13], but programming this process is challenging. The purposes of this paper are (a) to examine the effect of calorimeter time constant on single-injection ITC kinetic data, (b) to provide the user with information that can easily be used to predict the experimental conditions for optimum results, and (c) to describe methods and software for evaluating model parameters in mass-action kinetic models.

## 2. Effect of calorimeter time constant

The rate at which heat is generated by the reaction ($\phi_r$) is directly proportional to the reaction rate with $\Delta_R H$ as the proportionality constant. Observation of this heat rate by the calorimeter is delayed due to the effects of the time constant of the instrument as illustrated in Fig. 2. This delay manifests itself as the rising curve at small times and an elongation of the curve's tail at long times. For instruments with small time constants, this initial rise is sharp and brief and the exponential tail is mostly unaffected. However, for large time constants the initial rise can take a much longer time, resulting in a large elongation of the curve's exponential tail.

Often, only the decaying portion of the data in curves such as those in Fig. 2 have been analyzed to obtain kinetic constants with $\Delta_R H$ being determined from the area under the curve [2,4–6,8,14]. Only the exponential tail of the curve is fit because the instrument time constant is necessary to replicate the initial rising portion of the curve. This practice introduces new complications: How does one determine which data to ignore? And how much does the time constant affect these data where the signal is changing relatively rapidly? We illustrate this dilemma in Table 1 in which different portions of the real data in Fig. 1 are fit to Eqs. (3)–(6) with $\tau$ included or excluded as a fitting parameter. The second column

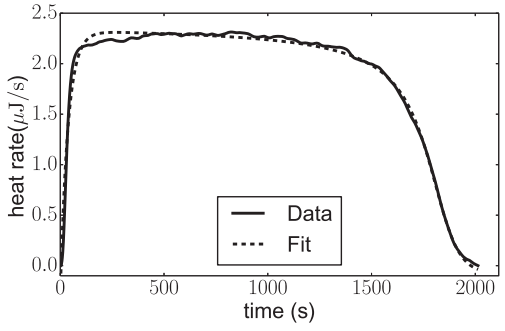


**Fig. 1.** Solid line – heat rate data from a single injection of 10 μL of 511 nM trypsin into 950 μL of 144 μM N-α-benzoyl-L-Arginine Ethyl Ester (BAEE) in 200 mM Tris–HCl buffer pH 8.0, 50 mM $CaCl_2$, and 0.2% PEG-2000 in an ITC model 2G (TA Instruments, Lindon, UT) [4]. Dashed line – fit to the data with Eqs. (3)–(6).

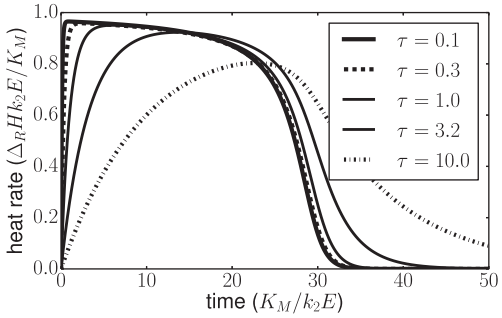


**Fig. 2.** Simulated Michaelis–Menten data for a single injection experiment in calorimeters with different time constants. Eqs. (3)–(6) were used to generate the curves.

**Table 1**
Inferred parameter values for the data in Fig. 1 for three different fitting schemes. Uncertainties are a 95% confidence interval derived from a maximum likelihood estimation of the noise in the data.

| Parameter | All data (Fit with $\tau$ as a fitting parameter) | Data for $t > 500$ with $\tau = 0$ | Data for $t > 1800$ with $\tau = 0$ |
|---|---|---|---|
| $k_2$ ($s^{-1}$) | 16.49 ± 0.04 | 16.290 ± 0.006 | 16.27 ± 0.06 |
| $K_M$ (μM) | 4.02 ± 0.14 | 4.28 ± 0.02 | 4.07 ± 0.10 |
| $\Delta_R H$ (kJ $mol^{-1}$) | 29.3 ± 0.4 | 29.45 ± 0.08 | 30.8 ± 1.0 |
| $\phi_B$[a] (μW) | 0.078 ± 0.026 | 0.0266 ± 0.0050 | 0.014 ± 0.056 |
| $\tau$ (s) | 37.1 ± 1.2 | n/a | n/a |

[a] $\phi_B$ is the baseline heat rate which was used as a fitting parameter in these calculations.

in Table 1 gives the results of fitting the data with the methods of references [7,9] in which the correction for the instrument time constant is explicitly included as a parameter. The third column gives the results of fitting with $\tau = 0$ and ignoring all data before the decaying part of the curve (i.e. at times >500 s, after the observed maximum heat rate). The last column gives the results of a more conservative fit using data only at times >1800 s (i.e., after the inflection point). The results from Table 1 indicate that inferred values of $k_2$ and $K_M$ vary with the subjective choice of which data to include. In particular, in this example $K_M$ changed by 5%. And, although $k_2$ changed by less than 1%, this change corresponds to >9 statistical standard deviations. Furthermore, because the ratio $k_2/K_M$ is small, the trypsin–BAEE system is a particularly forgiving system.

Fig. 3 explores the errors in inferred parameters for a range of values of $k_2$, $K_M$, $\Delta_R H$, and $\phi_B$ as functions of the fraction of completion of the reaction, $\alpha$. Artificial data are generated (without noise) for a fixed value of the instrument time constant. Data in the exponential tail are fit to Eqs. (3)–(6) with $\tau = 0$, thus ignoring the effects of instrument time constant. The $y$-axis is the dimensionless time scale of the Michaelis–Menten reaction, $k_2\tau E/K_M$, in units of the instrument time constant.

Notice in Fig. 3, a narrow, horizontal band of experimental conditions (defined primarily by the error in $K_M$) exists between $0.1/\tau$

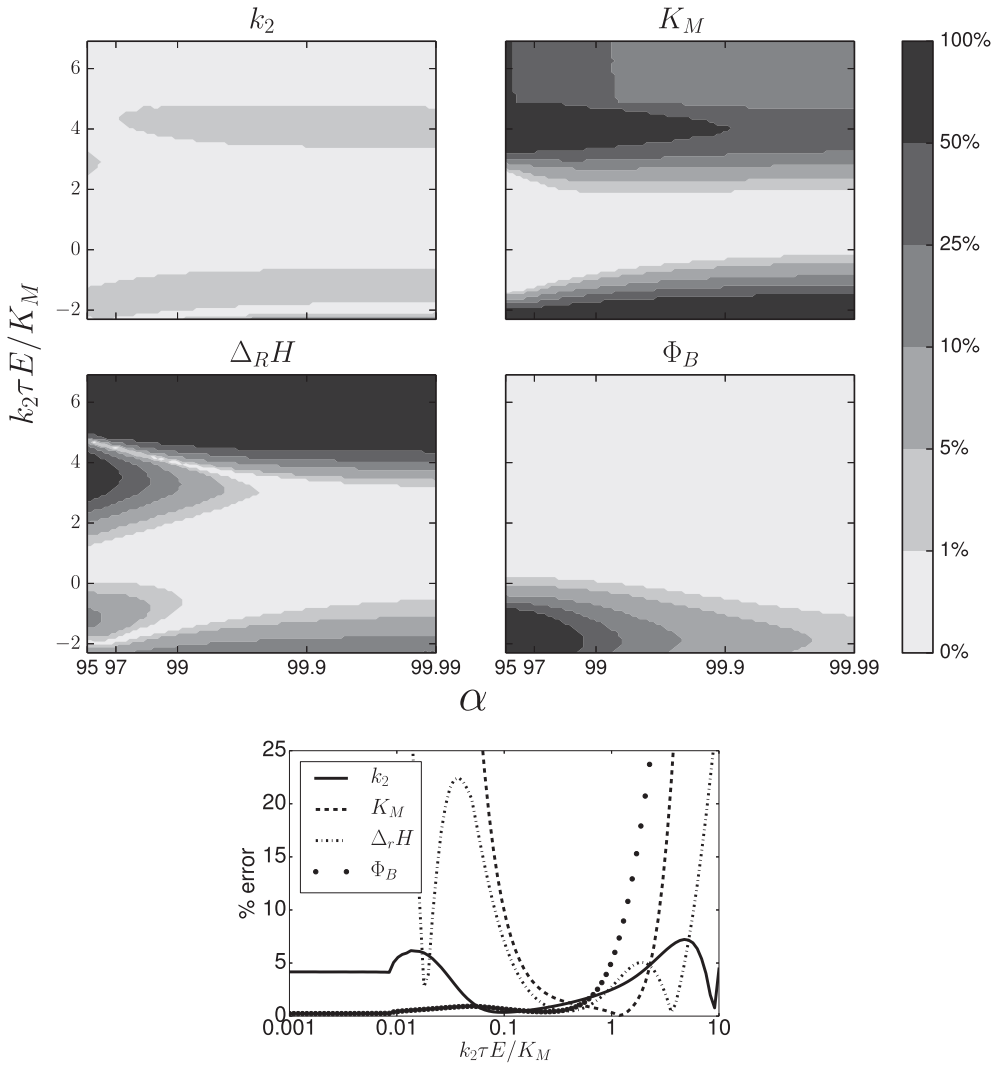


**Fig. 3.** Percent error in inferred parameters when fitting with $\tau = 0$. The line plots in the fifth panel show a slice through each of the other four panels at $\alpha = 99\%$.

and $1/\tau$ in which $\tau$ has negligible effects on all the parameters, $k_2$, $K_M$, $\Delta_R H$, and $\phi_B$. This band corresponds to $(0.1/\tau) < (k_2 E/K_M) < (1/\tau)$ with the reaction running to >99% completion (a limit set by error in $\Delta_R H$). Within this band of conditions, $k_2$, $K_M$, $\Delta_R H$, and $\phi_B$ can all be estimated with <1% error without correction for $\tau$. For experimental conditions outside of this band, the error in the inferred parameters grows quickly to unreasonable levels.

Returning to the experimental data in Fig. 2 and inferred parameter values in Table 1, the parameter that characterizes the reaction rate ($k_2 E/K_M$) has a value of 0.82, placing it near the upper boundary of acceptable conditions, consistent with the observations in Table 1. Had the experiment been conducted with a smaller enzyme concentration, thus reducing the reaction rate relative to the instrument time constant, the errors in the inferred parameters could have been reduced.

## 3. Selection of optimum conditions

Fig. 3 can be used to select the experimental conditions under which $k_2$, $K_M$, $\Delta_R H$, and $\phi_B$ can be accurately inferred from the decaying portion of the data without correcting for $\tau$. As a general rule, the reaction should be run to at least 99% completion and the value of $k_2 E/K_M$, which can be experimentally controlled by varying the concentration of the injected enzyme, must be chosen to lie within the optimal band of $0.1/\tau$ and $1/\tau$. However, application of this rule is complicated by the need to have reasonable *a priori* estimates of $k_2$, $K_M$, and $\tau$. Furthermore, there are no rigorous checks to determine if the inferred parameters are biased by the instrument time constant or the subjective choice of data.

A more rigorous approach is to explicitly include the effects of the instrument time constant in the model and include $\tau$ as an additional fitting parameter as described in references [7,9]. This procedure was used to calculate the values in the second column in Table 1. This mathematical model fits both the rising and falling parts of the observed heat rates (as in Fig. 2) and simultaneously provides estimates of all the relevant parameters (including the effective instrument time constant). With this model, standard statistical techniques can be applied to estimate the uncertainties in the inferred parameters. For example, the error bars for the inferred parameters can be found from the square roots of the diagonal entries of the inverse Fisher Information Matrix. Other techniques such as Bayesian MCMC or profile likelihoods can also be applied. These techniques overcome the problems described above by providing an explicit confidence interval for all the parameters, including the unknown effects of the instrument time constant.

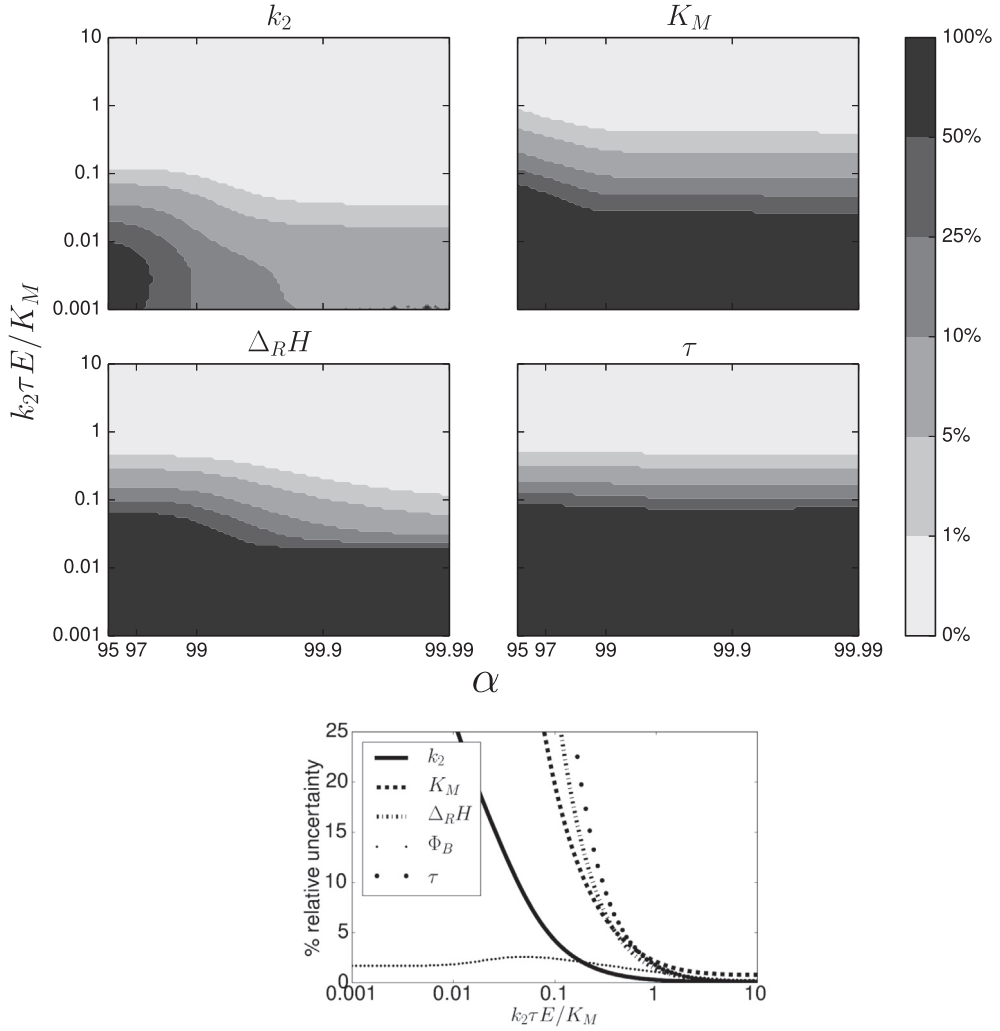


**Fig. 4.** Uncertainties in inferred parameters when including $\tau$ as a fitting parameter. The fifth panel shows line plots of a slice through each of the other four panels at $\alpha = 99\%$. The error bar estimated for the data in Fig. 1 is used for the parameter uncertainty for the artificial data in Fig. 4. We do not include the baseline parameter as it is accurately inferred provided the experiment is run long enough.

Repeating the process used to generate Fig. 3, but including the effects of the instrument time constant obviously allows the model to perfectly fit the simulated data. However, the previous analysis can be extended to estimate the statistical uncertainties in the inferred parameter values from the Fisher Information Matrix. The results are presented in Fig. 4 that shows the statistical uncertainties from noise in the data. In contrast, Fig. 3 illustrates the bias, i.e., errors, in $k_2$, $K_M$, $\Delta_R H$, and $\phi_B$ caused by use of an inaccurate model.

Note that Fig. 4 is unlike the conditions in Fig. 3. When $\tau$ is ignored, the optimal design corresponds to only a narrow band of reaction rates. Fig. 4 shows that the only condition that prevents obtaining good results is running the reaction at too fast a rate which causes the uncertainties in the inferred parameter values to become very large, i.e., the black regions in Fig. 4. In this regime, the temporal effects of the instrument time constant are functionally equivalent to changes in the reaction rate, leading to co-linearity among the parameters and large uncertainties. These large uncertainties are a feature rather than a problem of the present analysis. Experiments conducted in this regime are *uninformative* because they cannot discriminate between the kinetic properties of the reaction and the dynamical properties of the instrument. This fact cannot be seen unless the effects of the instrument time constant are explicitly included in the model.

Note that the plots in Figs. 3 and 4 represent two very different (but often conflated) ideas. Fig. 3 illustrates what we have called "error", that is, the systematic bias introduced to the parameter estimates because an inaccurate model was used. Fig. 4 illustrates what we have called "statistical uncertainty", and is the expected unbiased random errors introduced by fitting noisy data.

Fig. 4 can be used to determine optimal experimental conditions for inferring parameter values with $\tau$ as a fitting parameter. Fig. 4 indicates that all parameters can be accurately inferred provided the reciprocal of the reaction time constant ($k_2 E/K_M$) is larger

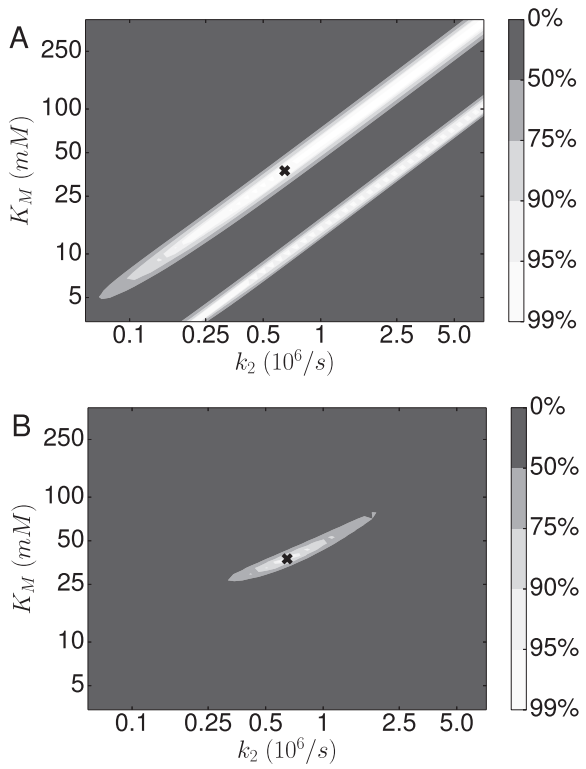


**Fig. 6.** Joint confidence regions for $k_2$ and $K_M$. (A) Statistical uncertainty from fitting the two data sets with sucrose concentrations of 0.25 and 2.5 mM. Any values of $k_2$ and $K_M$ with a ratio within the white area of the figure will fit these data, thus showing that accurate, independent values of these parameters cannot be obtained from these data. (B) Statistical uncertainty from a global fit to all six data sets with sucrose concentration $\geqslant$0.025 mM, showing that unique values of $k_2$ and $K_M$ can be obtained when data from an enzyme saturated condition are included.

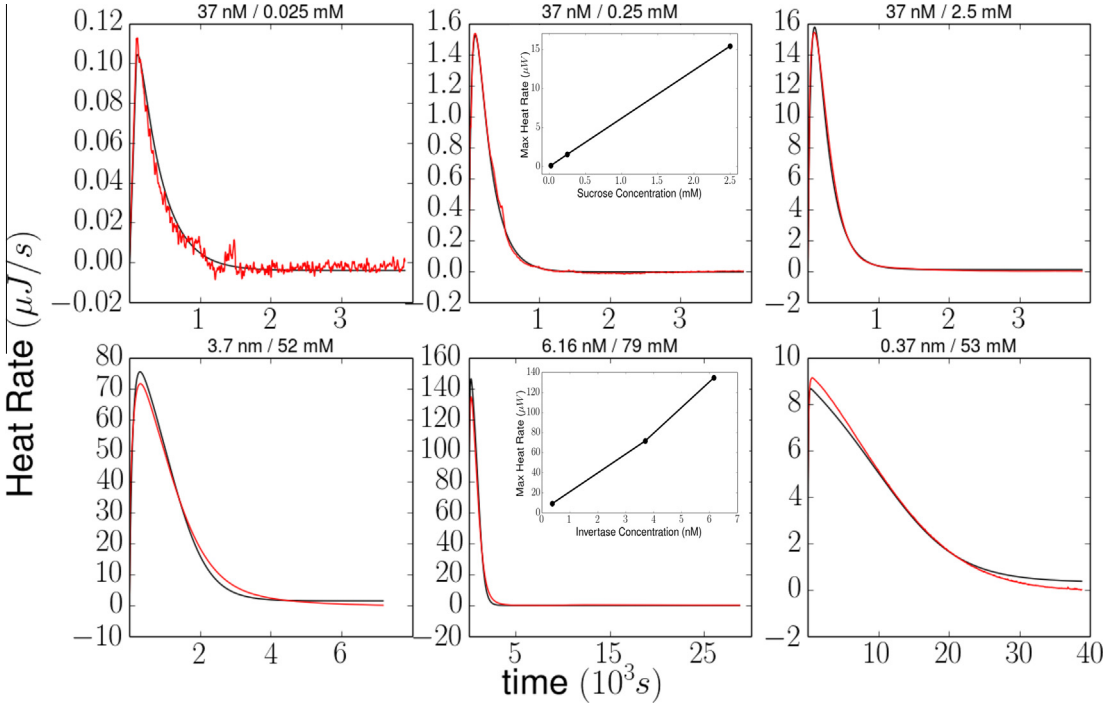


**Fig. 5.** Solid line – heat rate data from a single injection of 2 or 3 μL of buffer followed by 5 μL of invertase (grade VII from bakers yeast, Sigma, St. Louis, MO, 270 kD) into 164.5 μL of sucrose (EMD, Gibbstown, NJ) at 25 °C in 100 mM sodium acetate (minimum 99.0% Sigma, St. Louis, MO) buffer at pH 5.6. Data were collected with a NanoITC Low Volume calorimeter (TA Instruments, Lindon, UT). Dashed line – fit to the data with Eqs. (3)–(6). Values of $\Delta_R H$ calculated from integration of the data, and $\phi_B$ and $\tau$ from the global fit for each experiment are given in Table 3. The top inset plot of maximum heat rate versus sucrose concentration demonstrates the enzyme was not substrate saturated at sucrose concentrations $\leqslant$2.5 mM. In contrast, the bottom inset showing maximum heat rate versus invertase concentration demonstrates that saturation was achieved in the three experiments with sucrose concentration >50 mM.

than $1/\tau$. After values of $k_2$, $K_M$, $\Delta_R H$, and $\tau$ have been determined by fitting the data curve with Eqs. (3)–(6), the value of $\Delta_R H$ obtained can be verified by comparison with $\Delta_R H$ determined from the area under the curve.

In choosing optimal conditions, a further condition that must be satisfied is that data must be obtained so that the entire parameter space is adequately sampled. Consider two conditions, one where the enzyme is substrate-saturated (i.e., $S \gg K_M$) and another where $S \ll K_M$. The equations representing these two cases are

$$dS/dt = -k_2 E \text{ or } \phi_r(t) = -\Delta_R H V k_2 E \quad (7)$$

and

$$dS/dt \approx -k_2 ES/K_M \text{ or } \phi_r(t) \approx -\Delta_R H V k_2 ES/K_M \quad (8)$$

Eq. (7) shows that the measured heat rate depends only on $-\Delta_R H$, $k_2$ and $E$ under saturating conditions. Eq. (8) shows that the heat rate at half the maximum depends on $-\Delta_R H$, $k_2$, $E$ and the value of $K_M$. Note that conditions where $S << K_M$ are sampled only during the decaying portion of the data. To separate $k_2$ from $K_M$ and thus avoid the correlation between these parameters, requires the experiment to sample data from both conditions.

Achieving enzyme saturated conditions is particularly challenging for systems with a large value of $k_2/K_M$. Therefore we chose the invertase–sucrose system to further test the single injection method. Fig. 5 shows the results from injection of varying amounts of invertase into sucrose solutions with concentrations of sucrose ranging from 0.025 to 79 mM. Data were first collected at 0.025, 0.25, and 2.5 mM sucrose and 3.7 nM invertase in order to establish conditions for optimum results. Analysis of these data showed that saturation conditions were not sampled, see the inset in Fig. 5 that shows a linear dependence on sucrose concentration for these three experiments as required by Eq. (8). Thus $k_2$ and $K_M$ were not separable as shown by Fig. 6A. Fig. 6B explores the statistical uncertainty in the results from the global fit of all six data sets. Table 3 gives the experimental conditions for all six experiments and results for $\Delta_R H$ from integration of the area under each curve.

**Table 2**
Comparison of results from this study with results from the literature. Statistical uncertainties are given as 95% confidence intervals computed from the shape of the surface around the minimum.

| | Reference | $-\Delta_R H$ (kJ mol$^{-1}$) | $k_2$ (s$^{-1}$) | $K_M$ (μM$^{-1}$) | $\tau$ (s) | Conditions |
|---|---|---|---|---|---|---|
| Trypsin/BAEE | This work, fit to data from [4] | 29.3 ± 0.3 | 16.48 ± 0.03 | 4.02 ± 0.05 | 37.1 ± 0.4 | 5.4 nM trypsin, 200 mM Tris–HCl, pH 8.0, 50 mM $CaCl_2$, 0.2% PEG-2000, 25 °C, 144 μM BAEE |
| | [4] | 26.5 | 17.8 | 4.17 | | 5.4 nM trypsin, 200 mM Tris–HCl, pH 8.0, 50 mM $CaCl_2$, 0.2% PEG-2000, 25 °C, 144 μM BAEE |
| | [2] | 47.9 | 15 | 4 | | 9.6 nM trypsin, 200 mM Tris–HCl, pH 8.0, 50 mM $CaCl_2$, 0.2% PEG-8000, 25 °C, 171 μM BAEE |
| | [15] | | 22 | 5 | | pH 8, 50 mM $CaCl_2$, 25 °C |
| Invertase/ sucrose | Global fit, this work | 12.4 ± 0.01 | 647,000 ± 3000 | 37,500 ± 400 | See Table 3 | 100 mM acetate buffer, pH 5.6, 25 °C. See Table 3 for other concentrations |
| | [9] | 13.4 | 221,000 | 16,300 | 14.5 | 5 nM invertase, 100 mM acetate buffer, pH 5.65, 25 °C, 5 mM sucrose |
| | [16] | 15.4 | | 46,000 | | 50 mM acetate buffer, pH 4.6, 25 °C |
| | [17] | 14.93 | | | | 100 mM acetate buffer, pH 5.65, calorimetric determination |
| | [18] | | | 49,000 | | 100 mM acetate buffer, pH 4.5, 40 °C, (25, 50,1 00, and 200) mM sucrose |
| | [19] | | | 25,000 | | 0.1 or 0.05 μg/mL invertase, 200 mM acetate buffer, pH 4.9, 37 °C |
| | [20] | | | 52,900 | | 5–700 mM sucrose, 100 mM acetate buffer, pH 4.7, 30 °C |
| | [21] | | | 28,000 | | 0.1 μ/mL invertase, 25 mM acetate buffer, pH 5.0, 50 mM NaCl, 2 mM $NaN_3$ |
| | [22] | | | 331,000 | | (10, 6.67, 5, 3.33, 2.5) g/dL sucrose, 22 °C, 132 mM phosphate buffer, pH 7.0 |
| | [23] | | 367–450 | 64,000–110,000 | | Acetate buffer, pH 4.9 |
| | [24] | | | 28,700 | | From literature |
| | [25] | | | 140,000 | | (0.100, 0.271, 0.427, 1.36, 1.50, 2.00) M sucrose, 25 °C, citrate buffer, pH 5.0 |
| | [26] | | | 140,000 | | 0.1–1 M sucrose, 25 °C, pH 5 |
| | [27] | | | 160,000 | | 0.04–2.06 M sucrose, 25 °C, phosphate buffer, pH 5 |
| | [28] | | | 16,700 | | |

**Table 3**
Conditions for sucrose–invertase experiments. All experiments were run at 25 °C in 100 mM acetate buffer at pH 5.6 with a 5 μL injection of invertase into 164.5 μL of sucrose. The value of $\Delta_R H$ for individual experiments is calculated from integration of the area under the curve with $\phi_B = 0$. The% error in $\Delta_R H$ is calculated assuming a value of −14.93 kJ/mol from [17]. Values of $\tau$ and $\phi_B$ in the table are from the global fit of data from all six experiments allowing for differing values for these parameters among experiments. Uncertainties are given as 95% confidence intervals computed from the shape of the surface around the minimum.

| [invertase] in buret (nM) | [invertase] in cell (nM) | [sucrose] before injection (mM) | [sucrose] after injection (mM) | μmole sucrose | mJ from integration[a] | $-\Delta_R H$ (kJ mol$^{-1}$) sucrose | % error in $\Delta_R H$ | $\tau$ (s) | $\phi_B$ (μW) |
|---|---|---|---|---|---|---|---|---|---|
| 3.7 | 0.112 | 0.025 | 0.02394 | 0.003937 | – | – | – | 330 ± 1 | 0.004 ± 0.000 |
| 3.7 | 0.112 | 0.25 | 0.2394 | 0.03937 | 0.5215 | 13.24 | −11 | 208 ± 1 | 0.006 ± 0.001 |
| 3.7 | 0.112 | 2.5 | 2.394 | 0.3937 | 5.444 | 13.83 | −7 | 199 ± 1 | −0.09 ± 0.01 |
| 0.37 | 0.0112 | 53 | 50.44 | 8.294 | 114.7 | 13.83 | −7 | 90 ± 1 | −1.38 ± 0.04 |
| 3.7 | 0.112 | 52 | 49.49 | 8.138 | 110.3 | 13.55 | −9 | 75 ± 1 | 0.12 ± 0.07 |
| 6.16 | 0.187 | 79 | 75.19 | 12.36 | 153.6 | 12.43 | −17 | 75 ± 2 | −0.33 ± 0.01 |
| | | | | | | Mean $-\Delta_R H$ = 13.4 ± 1.2 | | | |
| | | | | | | Global fit $-\Delta_R H$ = 12.4 ± 0.01 | | | |

[a] A blank correction of 12.16 μJ determined by injection of 3 μL of buffer followed by 5 μL of invertase into buffer was subtracted from the total heat.

A global fit of the data with sucrose concentrations from 0.025 to 79 mM produces values of $k_2$, $K_M$ and $\Delta_R H$ with small statistical uncertainties, see Table 2.

Conditions that would provide a long, relatively flat plateau region, as in Fig. 1 for trypsin–BAEE, are not accessible for the invertase–sucrose system because enzyme concentrations below 3.7 nM gave too small heat rates and sucrose concentrations above 79 mM were too viscous. Therefore we chose to demonstrate that saturation was achieved by demonstrating a linear relation between maximum heat rate and invertase concentration as required by Eq. (7), see the inset in Fig. 5. When sucrose concentration is $\geqslant$50 mM the linear relation shows that saturated conditions were sampled, i.e., Eq. (7) indicates that the maximum heat rate depends only on the enzyme concentration and has no dependence on substrate concentration.

## 4. Results and discussion

The possibility of product inhibition at high concentrations of sucrose was examined with a global fit of the six data sets in Fig. 5A with Eq. (9).

$$dS/dt = -[k_2 ES/(K_M + S)] + [k_i(S_0 - S)] \quad (9)$$

The results gave $k_i = 0$, showing the absence of product inhibition in these experiments. These results differ from some results in the literature because of differences in conditions or invertase preparation.

Note that $\tau$ in Table 3 is much larger for the three experiments with low sucrose concentrations than for the three runs with high sucrose concentrations although all six experiments were done in the same calorimeter. The difference in the value of $\tau$ is a consequence of differing relative densities of the solutions in the cell and in the burette. The density of the titrant is higher than the density of the sucrose solution at low concentrations of sucrose and mixing time is increased because the titrant flows to the bottom of the cell before being mixed. At high concentrations of sucrose, the titrant is less dense than the sucrose solution, flows upward through the stirrer as it is injected, and therefore mixing time is greatly shortened. This result further demonstrates that $\tau$ is not a constant and cannot be determined with a heater pulse or methanol injection.

Table 2 compares the results from this study with previously published results on trypsin–BAEE and invertase–sucrose. The only notable difference between our results on trypsin–BAEE and literature results is the $\Delta_R H$ value reported by Todd and Gomez [2], $\Delta_R H = -47.9$ kJ/mol, which is approximately double the $\Delta_R H$ values reported by other workers. Todd and Gomez [2] state "the raw data... were corrected for the instrument response time" which "had a small effect on rate values" but give no details, and further state "the time course over which the enzyme reaction rate decays to zero is much larger than the instrument time constant (typically 10–20 s)" which implies that only the decaying portion of the data was analyzed for kinetic parameters and $\Delta_R H$ was obtained by integration of the area under the curve. For the invertase–sucrose system, the most accurate value for $\Delta_R H$ is probably that of Goldberg. Compared with Goldberg's value, the $\Delta_R H$ values from this study and from Demarse are both about 10% low, and that of Hüttl, about 3% high. Note that the values of $\Delta_R H$ from area integration and from the global fit are in agreement. The low value of $\Delta_R H$ from this study is likely caused by errors in the baseline correction ($\approx$8%) and in the calibration of the very small cell volume ($\approx$2%). Differences in $k_2$ and $K_M$ values in Table 2 are likely caused by differences in conditions and invertase preparations.

## 5. Conclusions

In conclusion, assuming that a correct and complete model for all of the reactions in the system is applied and that optimal experimental conditions are chosen, fitting single injection kinetic data with the method described in this paper produces accurate results for $k_2$, $K_M$, $\Delta_R H$, $\tau$ and $\phi_B$. The two systems included in this study represent extreme cases for the ratio of $k_2/K_M$; this ratio equals 4 $s^{-1}/\mu M^{-1}$ for the trypsin–BAEE system and 17 $s^{-1}/\mu M^{-1}$ for the invertase–sucrose system. Enzyme saturated conditions are easily achieved with systems with a small value of this ratio, but only with difficulty for systems with large values of this ratio. Enzyme saturated conditions must be achieved in order to obtain accurate values for $k_2$ and $K_M$, otherwise these two parameters are highly correlated and data can be fit with any values that provide the ratio required by the minimum in the fitted surface.

## Acknowledgement

The authors acknowledge and appreciate useful discussions of the mathematics with Clifford W. Hansen.

## References

[1] A.S. Futran, A.J. Link, R. Seger, S.Y. Shvartsman, Curr. Biol. 23 (2013) R972–R979.
[2] M.J. Todd, J. Gomez, Anal. Biochem. 296 (2001) 179–187.
[3] S.N. Olsen, Thermochim. Acta 448 (2006) 12–18.
[4] C.T. Choma, Charaterizing enzyme kinetics by ITC, Applications Note, TA Instruments, New Castle, DE.
[5] M.L. Bianconi, J. Biol. Chem. 278 (21) (2003) 18709–18713.
[6] P.E. Morin, E. Friere, Biochemistry 30 (1991) 8494–8500.
[7] C.W. Hansen, L.D. Hansen, A.D. Nicholson, M.C. Chilton, N. Thomas, J. Clark, J.C. Hansen, Int. J. Chem. Kinetics 43 (2) (2011) 53–61.
[8] D. Burnouf, E. Ennifar, S. Guedich, B. Puffer, G. Hoffmann, G. Bec, F. Disdier, M. Baltzinger, P. Dumas, J. Am. Chem. Soc. 134 (2012) 559–565.
[9] N.A. Demarse, M.C. Killian, L.D. Hansen, C.F. Quinn, Methods Mol. Biol. 978 (2013) 21–30.
[10] M.K. Transtrum, B.B. Machta, J.P. Sethan, Phys. Rev. Lett. 104 (2010) 1060201.
[11] Transtrum M.K., Geodesic Levenberg–Marquadrt Source Code, 2012. <http://sourceforge.net/projects/geodesiclm/>.
[12] M. Goličnik, Anal. Biochem. 406 (2010) 94–96.
[13] R. Ghai, R.J. Falconer, B.M. Collins, J. Mol. Recognit. 25 (2012) 32–52.
[14] K.A. Vander Meulen, S.E. Butcher, Nucleic Acids Res. 40 (2012) 2140–2151.
[15] T. Inagami, J. Biol. Chem. 239 (1964) 787–791.
[16] R. Hüttl, K. Ochlschläger, G. Wolf, Thermochim. Acta 325 (1999) 1–4.
[17] R.N. Goldberg, Y.B. Tewari, J.C. Ahluwalia, J. Biol. Chem 264 (1989) 9901–9904.
[18] D. Combes, P. Monsan, Carbohydrate Res. 117 (1983) 215–228.
[19] K.E. Shearwin, D.J. Winzor, Arch. Biochem. Biophys. 260 (1988) 532–539.
[20] V. Štefuca, A. Welwardová, P. Gemeiner, Anal. Chim. Acta 355 (1997) 63–67.
[21] F. Exnowitz, B. Meyer, T. Hackl, Biochim. Biophys. Acta 2012 (1824) 443–449.
[22] P. Heinzerling, F. Schrader, S. Schanze, J. Chem. Educ. 89 (2012) 1582–1586.
[23] J.D. Kehlbeck, C.C. Slack, M.T. Turnbull, S.J. Kohler, J. Chem. Educ. 91 (2014) 734–738.
[24] M. Goličnik, Comput. Chem. 70 (2013) 63–72.
[25] B.W. Imison, R.Y.K. Yang, Chem. Eng. Commun. 6 (1980) 151–160.
[26] J. López Santín, C. Solà, J.M. Lema, Biotechnol. Bioeng. 24 (1982) 2721–2724.
[27] L. Bowski, R. Saini, D.Y. Ryu, W.R. Vieth, Biotechnol. Bioeng. 13 (1971) 641–656.
[28] K.A. Johnson, R.S. Goody, Biochem. 50 (2011) (1913) 8264–8269.